Abundances of the Cosmic Ray β-decay Secondaries and Implications for Cosmic Ray Transport

N. E. Yanasak[1], W. R. Binns[2], E. R. Christian[3], A. C. Cummings[4], A. J. Davis[4], J. S. George[4], P. L. Hink[2], J. Klarmann[2], R. A. Leske[4], M. Lijowski[2], R. A. Mewaldt[4], E. C. Stone[4], T. T. von Rosenvinge[3], M. E. Wiedenbeck[1]

[1]*Jet Propulsion Laboratory*
[2]*Washington University*
[3]*NASA/Goddard Space Flight Center*
[4]*California Institute of Technology*

Abstract. Galactic cosmic rays (GCRs) pass through the interstellar medium (ISM) and undergo nuclear interactions that produce secondary fragments. The abundances of radioactive secondary species can be used to derive a galactic confinement time for cosmic rays using the amount of ISM material traversed by the cosmic rays inferred from stable GCR secondary abundances. Abundance measurements of long-lived species such as ^{10}Be, ^{26}Al, ^{36}Cl, and ^{54}Mn allow a comparison of propagation histories for different parent nuclei. Abundances for these species, measured in the energy range $\sim 50 - 500$ MeV/nuc using the Cosmic Ray Isotope Spectrometer (CRIS) aboard the Advanced Composition Explorer (ACE) spacecraft, indicate a confinement time $\tau_{esc} = 16.2 \pm 0.8$ Myr. We have modeled the production and propagation of the radioactive secondaries and discuss the implications for GCR transport.

INTRODUCTION

The abundances of secondary cosmic rays, produced by fragmentation of primary galactic cosmic rays (GCRs) as they pass through the interstellar medium (ISM), are a measure of the amount of material through which the GCRs pass before escaping from the galaxy. The value of the average pathlength before escape at a particular GCR energy λ_{esc}, determined by measurements of the ratio of secondary to primary GCR abundances, corresponds to an ISM density ρ_{ISM} and a propagation time in the galaxy τ_{esc} (confinement time). Within the "leaky box" model (LBM), the relationship between these three quantities and GCR velocity v is assumed to be $\lambda_{esc} = \rho_{ISM} v \tau_{esc}$. The radioactive β-decay secondaries will undergo decay after production during propagation and serve as "clocks", measuring the average rate of escape in comparison to the decay time. Therefore, the surviving abundance of these species will be sensitive to τ_{esc} and the ISM density. Abundances reported from the IMP-7,8 and ISEE-3 spacecraft were consistent with a mean ISM number density $n_{ISM} \sim 0.1 - 0.3$ atoms/cm^3 and τ_{esc} between 6-20 Myr (for a review, see (1)). Precise measurements of ^{26}Al, ^{36}Cl, and ^{54}Mn which allow for a comparison of propagation histories for different parent nuclei have been made recently by several experiments (2, 3), leading to improved values for τ_{esc} and the average ISM density characteristic of the cosmic ray confinement region.

Interpretation of the secondary radionuclide abundances is specific to the framework of the chosen propagation model. The LBM replaces the spatial diffusion and loss of particles at the galaxy boundary in more complex models by a mean energy-dependent, spatially-independent escape pathlength. Despite the simple nature of the LBM, its predictions can be made to fit a variety of GCR abundance measurements. The LBM is a suitable approximation to more realistic propagation models which may incorporate diffusion, convection, and reacceleration of the GCRs (e.g., (4)). However, differences between these models arise in the predictions for the shorter halflife radioactive species if one assumes inhomogeneities in the local ISM. We report new measurements of the β-decay secondaries and attempt to provide a consistent picture of GCR propagation for all the secondary radionuclides using our steady state LBM and predictions from other models.

OBSERVATIONS

The data reported here were obtained using the Cosmic Ray Isotope Spectrometer (CRIS) instrument aboard

CP528, *Acceleration and Transport of Energetic Particles Observed in the Heliosphere: ACE 2000 Symposium,*
edited by Richard A. Mewaldt, et al.

the Advanced Composition Explorer (ACE) spacecraft (5). This instrument uses the dE/dx versus total E technique to measure elemental and isotopic composition of the galactic cosmic rays. It consists of four Si detector stacks to measure the particle energy deposition and a scintillating optical fiber trajectory (SOFT) hodoscope that acts as part of the trigger and determines particle trajectories (6). The period of observation for these data is between 27 August 1997 and 10 April 1999, excluding periods of significant solar energetic particle intensity. Events were selected for this study using charge and mass consistency requirements and a cut to reject particles stopping near the edge or the surfaces of the silicon detectors where there are larger uncertainties in their identification (6).

The ratios of the radioactive isotope abundances to the abundances of stable isotopes of the same elements are shown in Table 1. The isotopic abundances for Al, Cl, and Mn were determined using a maximum likelihood fit of Gaussian peaks to their mass histograms. Isotopes of Be are clearly resolved and their abundances were obtained by counting events in each peak (see (6)). The mass resolution of the Si detectors degrades with increasing angle of incidence because of multiple Coulomb scattering, and zenith angle cuts were applied for improved resolution of the mass peaks (6). Corrections to these abundances (<6% for all isotopes) were made to account for differences in fragmentation, SOFT detection efficiency, and geometry factor for a given energy interval.

Table 1. GCR Radionuclide Abundances from CRIS

Ratio	Energy (MeV/nuc)	Measurement
^{10}Be/^{9}Be	70-145	0.120±0.008
^{26}Al/^{27}Al	125-300	0.048±0.002
^{36}Cl/Cl	150-350	0.062±0.008
^{54}Mn/Mn	178-400	0.114±0.006

PROPAGATION MODEL

The observed abundances from CRIS were compared with model abundances calculated using a steady state LBM described in Yanasak, et al.(6). Our model source abundances were based on solar system isotopic observations (7) in conjunction with a source composition from HEAO-3 observations for predominant elemental species (e.g., C, Fe) (8) and Ulysses for rarer elemental species (e.g, P) and for ^{22}Ne (9), adjusted to match the CRIS data. Source spectra J were assumed to be power laws in momentum p: $dJ/dE \propto p^{-2.35}$. Energy loss, nuclear decay, spallation, and attachment and stripping of electrons from the GCR nuclei during propagation were considered in the model. The ISM composition was chosen to be 90% H, 10% He by number, with a 24% ionized H fraction.

The value of the escape length λ_{esc} was adjusted to match the CRIS data for the secondary to primary ratios B/C, F/Ne, P/S, and (Sc+V)/Fe as well as the ratio of elements for charges Z=17-25 to Fe to sample the secondary production for Cl. We assumed this following form of the escape length, motivated by the form given in (10):

$$\lambda_{esc} = \frac{28.0\beta}{(\beta R)^{0.6} + \alpha(\beta R/1.4GV)^{-1.4}} \qquad (1)$$

where R is the particle rigidity, α is a normalization factor, and β is the ratio of the particle velocity to the speed of light v/c. Previous low energy experiments which have measured secondary to primary ratios at multiple energies indicate a dependence of $\beta^{3.5-4.5}$ to fit the data over the full range in energy space (e.g., (11)) rather than the $\beta^{1.0}$ dependence commonly used in other studies (10). At lower energies, our form for λ_{esc} gives a dependence $\propto \beta(\beta R)^{1.4}$, and this strong dependence on energy provides a good fit for CRIS GCR secondary to primary ratios (6).

Although a value of $\alpha = 1.0$ provides a good fit for secondary to primary ratios with $Z < 21$, we were unable to account for all of the secondary to primary ratios with a unique value of α. Using α=1.0 tends to underestimate the production of sub-iron secondaries by ~15% at CRIS energies, while model predictions at higher energies are in good agreement with HEAO-3 data. For this study, we adjust λ at low energies for each clock species to match the secondary to primary ratios for parent nuclei which contribute most to that species, setting α=0.15 for ^{54}Mn analysis and α=1.0 for the other species.

Solar modulation of the cosmic ray spectra was simulated using a spherically symmetric model (12), with a diffusion coefficient proportional to βR. The diffusion coefficient used corresponds to a modulation parameter value of ϕ=325 MV (6).

DISCUSSION

Figure 1 shows a comparison between CRIS abundances for the secondary radionuclides measured at Earth and those obtained previously from Ulysses (13, 2, 14, 15), ISEE-3 (16, 17) and Voyager (18, 19, 20). Curves of constant ISM hydrogen density $n_H = n_{ISM} - n_{He}$ from our model calculations are shown overlying the data in Figure 1. Previously reported abundances were measured at different levels of solar modulation, and these have been adjusted to the level of modulation appropriate to CRIS for direct comparison. The largest adjustment required was 25% for the ISEE-3 measurement of ^{10}Be (17). Pre-

vious observations were reported as one value per experiment averaged over a wide energy range, owing to the limited counting statistics. Because of the larger number of events that CRIS collects, the data can be divided into several energy intervals, enabling comparisons with the predicted energy dependence. To within statistical uncertainties, the CRIS results are consistent with those reported from previous experiments. Because of the excellent statistical significance of the CRIS data, the effect of uncertainties in solar modulation on model predictions must be considered. A change in the solar modulation level $\Delta\phi \sim 50$ MV corresponds to a variation in the ISM number density of $\sim \pm 7\%$ from the ^{10}Be data and somewhat smaller variations for the other species (6).

From Figure 1, the observations imply $n_H = 0.28 - 0.43$ H atoms/cm^3. Differences in these results for n_H and those presented previously (3) are primarily due to the use of different total and partial fragmentation cross-section formulas (6). Average total ISM density values indicated by the secondary clock abundances are somewhat less than the typical assumption of a nominal ISM density in the galactic disk $n_{ISM} \sim 1$ atom/cm^3. Taken together, these four clock species indicate a hydrogen density $n_H \sim 0.34 \pm 0.02$ H atoms/cm^3, which is consistent to within two standard deviations for all four species. A systematic uncertainty in the halflife of ^{54}Mn must also be considered. From the combined observations of Wuosmaa, et al.(22) and Zaerpoor, et al.(23), the halflife of GCR ^{54}Mn is $6.8 \pm 1.5 \times 10^5$ yr. The size of this systematic uncertainty in determining n_H is comparable in amount to the statistical uncertainty shown for each CRIS ^{54}Mn data point in Figure 1. The abundance for the shorter-lived species ^{36}Cl does not indicate an ISM density which is significantly different than those implied by the other radioactive secondary abundances which sample a larger volume around the solar system. The densities indicated by the GCRs may imply significant propagation in a lower density galactic halo or propagation in a local ISM cavity (4).

The increase of the clock isotope abundances with increasing energy predicted by our LBM propagation model is consistent with the observed abundances of all clock species within the statistical limitations of the data. However, the data are also consistent with calculations from the diffusion model of Strong and Moskalenko (24), which shows a flatter energy dependence at CRIS energies. Variations in the energy dependence can result from the energy dependence in the isotopic fragmentation cross sections, which may contribute as much as 10% uncertainty to the predicted ISM density at the lowest energies probed by the CRIS data and less uncertainty at higher energies where more cross-section measurements have been made (6). Both the energy dependence and the value of the calculated density are dependent on the cho-

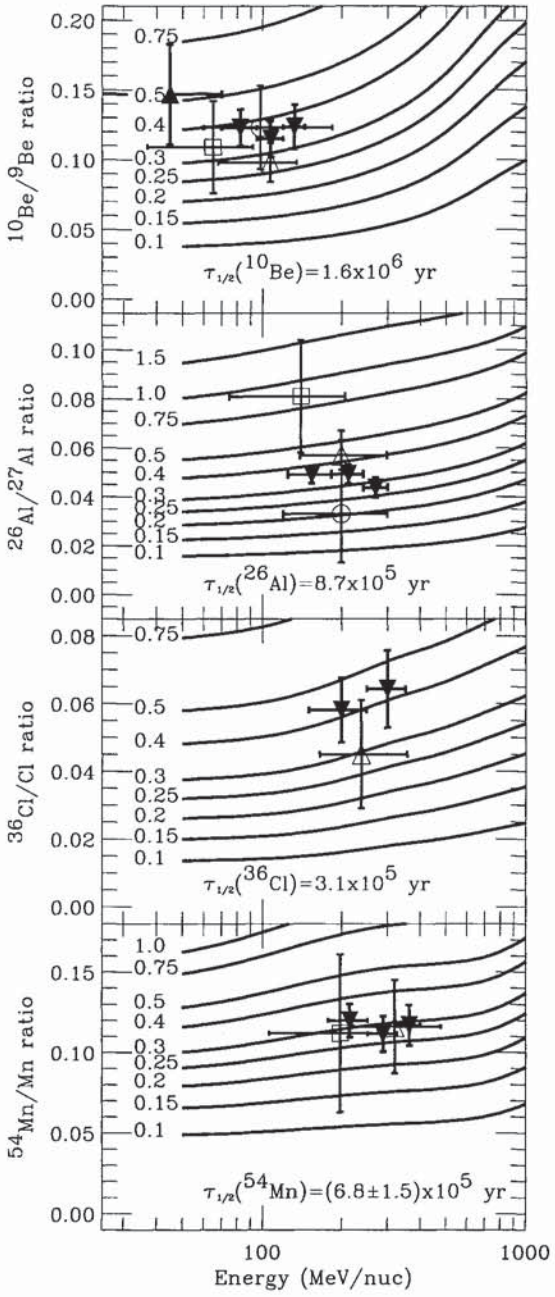

FIGURE 1. Secondary radionuclide abundance ratios from CRIS and previous experiments. Curves show predicted abundance ratios for different n_H in atoms/cm^3. An ISM helium component of n_{He}/n_H=0.11 has been assumed. Ratios from previous experiments have been adjusted to a level of solar modulation ϕ=325 MV for comparison. References for the data are as follows: *Filled triangle* this work; *Open circle* (16, 17); *Open square* (19, 18); *Open triangle* (13, 2, 14, 15)

sen parameterization of λ_{esc} within the formalism of the LBM.

Using the appropriate value of ρ_{ISM} for each species, the confinement times and statistical uncertaintites calculated from the CRIS clock abundances are presented in Table 2 along with previous results for comparison. The CRIS data imply a confinement time of $\tau_{esc} = 16.2 \pm 0.8$ Myr. This value is consistent with results from all four clock abundances to within two standard deviations, considering the systematic uncertainty in the halflife of ^{54}Mn in addition to the statistical uncertainty shown in Table 2. It should be noted that the CRIS abundance for ^{54}Mn is in good agreement with the Ulysses result (15). Although measured abundances from Ulysses and CRIS generally agree for all four clock species (Figure 1), the derived confinement times for ^{10}Be and ^{54}Mn are in slight disagreement. However, the higher value of τ_{esc} from ^{10}Be data measured by Ulysses cannot be explained by a difference in λ_{esc} in the respective models. We find $\lambda_{esc} \sim 6.7$ g/cm^2 from our model, which is higher in value than the pathlength used in the Ulysses analysis ($\sim$6.0 g/cm^2) and which should predict a higher value of τ_{esc} for similar ISM densities. This difference may result in part from a difference in partial fragmentation cross sections in the respective models.

Table 2. GCR Confinement Time

Clock	Experiment	τ_{esc}*(Myr)
^{10}Be	ACE/CRIS	$14.9^{+1.4}_{-1.2}$
	Ulysses (13)	$26.0^{+4.0}_{-5.0}$
	Voyager (19)	$27.0^{+19.0}_{-9.0}$
	ISEE-3 (16)	$8.4^{+4.0}_{-2.4}$
^{26}Al	ACE/CRIS	$18.0^{+1.2}_{-1.1}$
	Ulysses (15)	$19.0^{+3.0}_{-3.0}$
	Voyager (18)	$13.5^{+8.5}_{-4.5}$
	ISEE-3 (17)	$9.0^{+20.0}_{-6.5}$
^{36}Cl	ACE/CRIS	$13.8^{+2.5}_{-2.0}$
	Ulysses (2)	$18.0^{+10.0}_{-6.0}$
^{54}Mn	ACE/CRIS	$33.7^{+3.7}_{-3.2}$
	Ulysses (2)†	$\sim 11.0^{+4.7}_{-3.1}$

* The confinement times from experiments other than CRIS are compiled from the listed references.

† Recalculated from (14) using $\tau_{1/2} = 0.63$ Myr from (22).

CONCLUSION

Average ISM hydrogen number densities between $n_H = 0.28 - 0.43$ H atoms/cm^3 are necessary to account for the secondary radionuclides produced during propagation within the context of the leaky box model. A value of n_H=0.34±0.02 H atoms/cm^3 is consistent with all species to within two standard deviations. The surviving fractions of the secondary radionuclides indicate a mean confinement time for cosmic rays in the galaxy of $\tau_{esc} = 16.2 \pm 0.8$ Myr.

ACKNOWLEDGMENTS

This research was supported by the NASA at the California Institute of Technology (under grant NAG5-6912), the Jet Propulsion Laboratory, NASA/Goddard Space Flight Center, and Washington University.

REFERENCES

1. Simpson, J. A., *Ann. Rev. Nucl. Part. Sci.* **33**, 323 (1983).
2. Connell, J. J., DuVernois, M. A., & Simpson, J. A., *Ap. J. Lett.* **509**, L97 (1998).
3. Yanasak, N. E. et al., *Proc. 26th Int. Cosmic Ray Conf.* (Salt Lake City) **3**, 9 (1999).
4. Ptuskin, V. T., & Soutoul, A., *A&A* **337**, 859 (1998).
5. Stone, E. C. et al., *Space Sci. Rev.* **86**, 285 (1998).
6. Yanasak, N. E. et al., *Ap. J.* (in preparation) (2000).
7. Anders, E. & Grevesse, N., *Geochim. Cosmochim. Acta* **53**, 197 (1989)
8. Englemann, J.J., et al, *A&A*, **233**, 96 (1990)
9. DuVernois, M. A., and Thayer, M. R., *Ap. J.* **465**, 982 (1996).
10. Soutoul, A., and Ptuskin, V. T., *Proc. 26th Int. Cosmic Ray Conf.* (Salt Lake City) **4**, 184 (1999).
11. Krombel, K. E., & Wiedenbeck, M. E., *Ap. J.* **328**, 940 (1988)
12. Fisk, L. A., *JGR*, **76**, 221 (1971)
13. Connell, J. J. *Ap. J.* **501**, L59 (1998).
14. DuVernois, M. A., *Ap. J.* **481**, 241 (1997).
15. Simpson, J. A., & Connell, J. J., *Ap. J.* **497**, L85 (1998).
16. Wiedenbeck, M. E., & Greiner, D. E., *Ap. J. Lett.* **239**, L139 (1980).
17. Wiedenbeck, M. E., *Proc. 18th Int. Cosmic Ray Conf.* (Bangalore) **9**, 147 (1983).
18. Lukasiak, A., McDonald, F. B., & Webber, W. R., *Ap. J. Lett.* **430**, L69 (1994).
19. Lukasiak, A., et al., *Ap. J.* **423**, 426 (1994).
20. Lukasiak, A., McDonald, F. B., & Webber, W. R., *Ap. J.* **448**, 454 (1997b).
21. DuVernois, M. A., Simpson, J. A., and Thayer, M. R., *A&A* **316**, 555 (1996).
22. Wuosmaa, A. H., et al., *Phys. Rev. Lett.* **80**, 2085 (1998)
23. Zaerpoor, et al., *Phys. Rev. Lett.* **82**, 2219 (1999)
24. Strong, A. W., and Moskalenko, I. V. *Proc. 26th Int. Cosmic Ray Conf.* (Salt Lake City) **4**, 255 (1999).